Preprints.org

Article

Understanding the Effects of Adding Metal Oxides to Bioplastic and Bioplastic Blends on the Mechanical and Rheological Behaviour, Wettability, and Photo-Oxidation Resistance

Elisabetta Morici [*] , Giuseppe Pecoraro , Sabrina Carola Carroccio , Elena Bruno , Paola Scarfato ,
Giovanni Filippone , Nadka Tz. Dintcheva [*]

Article

Understanding the Effects of Adding Metal Oxides to Bioplastic and Bioplastic Blends on the Mechanical and Rheological Behaviour, Wettability, and Photo-oxidation Resistance

Elisabetta Morici [1,2,*], Giuseppe Pecoraro [2], Sabrina Carola Carroccio [3,4], Elena Bruno [4,5], Paola Scarfato [6], Giovanni Filippone [7] and Nadka Tz. Dintcheva [2,,3*]

1 ATEN Center, Università di Palermo, Viale delle Scienze, Ed. 18, 90128 Palermo, Italy
2 Dipartimento di Ingegneria, Università di Palermo, Viale delle Scienze, Ed. 6, 90128 Palermo, Italy
3 CNR-IPCB, Unit of Catania, Via P. Gaifami 18, 95126 Catania, Italy
4 CNR-IMM, Via Santa Sofia 64, I-95123 Catania, Italy
5 Dipartimento di Fisica e Astronomia "Ettore Majorana", Università di Catania, Italy
6 Department of Industrial Engineering, University of Salerno, Via Giovanni Paolo II, Fisciano (SA), Italy
7 Dipartimento di Ingegneria Chimica, dei Materiali e della Produzione Industriale, Università degli Studi di Napoli Federico II, 80125 Naples, Italy

* Correspondence: e-mail: elisabetta.morici@unipa.it, nadka.dintcheva@unipa.it; Tel.: +3909123863704

Abstract: Biopolymers are of growing interest, but to improve some of their poor properties and performance, it is required the formulation of bio-based blends and/or adding of nanoparticles. For this purpose, in this work, two different metal oxides, such as zinc oxide (ZnO) and titanium dioxide (TiO_2), at different concentrations (0.5, 1 and 2 %wt.) have been added in polylactic acid (PLA) and polylactic acid/polyamide 11 (PLA/PA11) blends to establish their effects on solid-state properties, morphology, melt behaviour, and photo-oxidation resistance. It seems that the addition of ZnO in PLA leads to a significant reduction of its rigidity probably due to an inefficient dispersion in the melt state, while the addition of TiO_2 does not penalise PLA rigidity. Interestingly, the addition of both ZnO and TiO_2 in PLA/PA11 blend has a positive effect on the rigidity because of blend morphology refinement and leads to a slight increase in film hydrophobicity. The photo-oxidation resistance of neat PLA and PLA/PA11 blend is significantly reduced due to the presence of both metal oxides, and this must be considered when designing the potential applications. The last results suggest that both metal oxides could be considered as photo-sensitive degradant agents for biopolymer and biopolymer blends.

Keywords: biopolymers; biopolymer blends; metal oxides; morphology refinement; photo-sensitive degradant agents

1. Introduction

Metal oxide-based polymeric nanocomposites are a significant class of materials from a technological and scientific view. Incorporating metal-oxides into the polymer matrix could improve physicochemical properties such as mechanical, thermal, biological, electrical, optical, and superficial properties. [1-2] The resultant nanocomposites are principally employed as sensors, for the photodegradation of pollutants, in water treatment, in membrane and ion exchanger technologies, and as adsorbent medium. [3-6] Among the different metal oxides, zinc oxide (ZnO) and titanium dioxide (TiO_2) are largely used as fillers for polymer nanocomposite preparation. [7-8] Zinc oxide is a chemically accessible, low-cost, with a high redox potential, able to remove organic pollutants and acts as an anti-bacterial agent. [9-10]

Titanium dioxide (TiO_2) has been extensively researched due to its stable structure, non-toxicity, anti-corrosion properties, and high photocatalytic activity. Indeed, TiO_2, both with ZnO nanoparticles, shows photocatalytic activity because of a positive band position that generates holes

(h+) and electrons (e−) by molecular excitation under UV light, resulting then in the generation of hydroxyl radicals and reactive oxygen species which, in turn, can interfere with pollutants and bacterial metabolism inhibiting their growth or causing the bacterial death. [11-13]

Research community was focused on petroleum-derived polymer matrix. However, the traditional approach is not more sustainable because of the increase in plastic waste generation and accumulation, and the growing alarms about the environmental impact of chemicals from petrochemical resources. These nanocomposites are non-biodegradable and can take many years to decompose, leading to worrying pollution and concern for human health and ecosystem stability. [14] The breakdown of larger plastics released into the environment produces microplastics (MPs), i.e. plastic particles less than five millimetres long, that are harmful to living organisms. [14-15] In addition, the manufacture of petrochemicals affects the environment by adding contaminants to the air, water, and soil and emitting greenhouse gases that can contribute to global climate change. [16-17] These troubles combined with the shortage of oil resources, have motivated research in utilizing alternative sources of raw materials to produce a new class of polymers having natural origin and degradability. In particular, biopolymers are supposed to replace conventional polymeric matrix with the goal of zero-waste, lower energy requirement to manufacture, and zero-emission and no hazardous chemicals released during manufacturing processes. Moreover, biodegradable polymers are suitable for some biological and medical applications. [18-20]

Poly(lactic acid) (PLA), a linear aliphatic compostable polyester, is synthesized from renewable raw materials, and finds several applications in different fields due to its relatively low cost, safety, versatility, appealing mechanical properties, high clarity, and ease of processing. Furthermore, products coming from PLA degradation are safe for living entities and do not harm the environment. The main uses are in food packaging, medical, automotive, textile, and agriculture areas. [21-23] Moreover, the production of polylactic acid, according to the production technique by the company NatureWorks, is expected to result in a 68% reduction in the consumption of fossil fuels compared to conventional plastics. [24] Despite these advantages, some properties need to be improved to achieve widespread use in industrial manufacturing. Critical drawbacks are related to brittleness, proper barrier properties, low melt strength, and thermal stability, while the degradation rate is slower compared to other common natural organic wastes, such as food and yard waste. The addition of nanoparticles (NPs) proved to be a method to overcome some limitations: significant improvements were observed in hybrid PLA nanocomposites, even at very low nanofiller loadings. [25-27] Physical thermomechanical properties enhance above all when proper polymer–filler interactions or suitable filler distribution are achieved.

Another successful, solvent-free and cost-effective way to obtain improved properties of the material is blending polymers with complementary properties. Polyamide 11 (PA11) is a biobased polymer having a similar glass transition temperature and melting point to PLA and exhibiting chemical resistance, high ductility and impact strength and better thermomechanical properties compared to PLA, which makes it a suitable candidate for blending with PLA. [28-29] Although the energy demand for the production of PA11 is relatively high, it is lower than that of polyamide 66 (PA66) and other oil-based competitors in the same performance range, such as Polycarbonate (PC), polyamide 6 (PA6) or Poly(methyl methacrylate) (PMMA). [30] Adding nanoparticles to immiscible blends could improve even more properties.

In this work, we present data that can be useful for materials science, aiming to find solutions to overcome drawbacks that limit applications of biopolymer-based nanocomposites. We study different PLA-based nanocomposites obtained varying the metal oxide concentration as well as the type of matrix, i.e. pure PLA and PLA/PA11 blend. At first, PLA/PA11 blends were prepared by mixing different amounts of the two homopolymers. Finally, the fully bio-based blend (PLA 70 %wt. and PA11 30 %wt.) containing the investigated metal oxide (ZnO and TiO$_2$ at 0.5 %wt., respectively) was studied.

2. Materials and Methods

2.1. Materials

The PolyLactic Acid (PLA), used in this work, was a commercial extrusion sheet grade supplied by NatureWorks (Nebraska, USA, named PLA 2002D) with an average number molecular weight of about 121000 g/mol, a ratio of 96% L-lactide to 4% D-lactide units, melt flow index 6 g/10 min (230°C, 2.16Kg).

The polyamide used in this work was a Polyamide 11, PA11, (Nylon 11, pellets form, from Sigma Aldrich), with glass transition temperature Tg = 46 °C, melting temperature Tm = 198 °C and density ϱ = 1.026 g/cm3 at 25 °C; molecular weight Mw = 201.31 g/mol, MFI@235 °C/2.16 kg = 14.5 ± 1.2 g/10 min.

Zinc oxide (ZnO) nanopowder (<100 nm particle size) was purchased from Sigma Aldrich and used with any further purification. According to our previous investigations, ZnO nanoparticle size spanned a 100-200 nm range, with a mix of tubular and round-shaped forms. [31]

Titanium dioxide (TiO$_2$, AEROXIDE® TiO$_2$ P25) was purchased from Evonic and used with any further purification. Specific surface area (BET): 35 - 65 m^2/g; density: approx.140 g/l.

2.2. Melt Processing

Both biopolymers PLA and PA11 and metal oxides were vacuum-dried at 80 °C overnight before processing to avoid hydrolytic degradation during melt processing. Neat PLA, containing commercial metal oxides (ZnO and TiO$_2$) at varying amounts (0.5, 1, and 2 %wt.) and PLA/PA11 blends, containing 0.5%wt. of metal oxides were prepared by melt mixing using a Brabender PLA-330 internal mixer at 200 °C for 5 min at 50 rpm. To improve the ZnO and TiO$_2$ dispersion in PLA melt and PLA/PA11 blend melt, the samples were pre-mixed for 1 min, and then, ZnO was added, and the mixing continued for another 4 min.

Thin films, having a thickness of ca. 120 microns, requested for the characterizations were obtained by the hot compression molding process.

2.3. Characterizations

FTIR Spectroscopy

A Fourier Transform Infrared Spectrometer (Spectrum One, Perkin Elmer) was used to record IR spectra using 16 scans at a resolution of 1 cm-1. The progress of photo-oxidation degradation of the samples has been followed by FTIR analysis monitoring the variations of carbonyl range (1850-1600 cm-1) in time, using Spectrum One software.

Water Contact Angle (WCA)

The water contact angle (WCA) was measured at room temperature using First Ten Angstrom (USA) FTA1000C system (Data Physics Instruments, Filderstadt, Germany), with demineralized water. The films were fixed on top of a plane solid support and kept flat during water deposition and acquisition. The sessile drop method was used with a droplet volume of 6 μL.

Tensile tests

Tensile tests were carried out using a universal testing machine (Instron model 3365, UK), according to the ASTM D882 method, on rectangular samples. The tests were performed using a tensile speed of 1 mm/min for 1 minute to evaluate the Young's modulus, and then the velocity was increased to 10 mm/min until sample breakage.

Rheological analysis

Rheological tests were performed using a stress-controlled rheometer (ARES G-2) in parallel plate geometry (plate diameter 25 mm). The complex viscosity (η^*), storage (G') and loss (G'') moduli were measured under frequency scans from ω = 10-1 to 100 rad/s at T = 170 °C. The strain amplitude was γ = 5%, which preliminary strain sweep experiments proved to be low enough to be in the linear viscoelastic regime.

Scanning Electron Microscopy (SEM)

The morphologies of the blend nanocomposites were investigated by scanning electron microscopy images (SEM, Gemini 152 field emission SEM Supra 25, Carl Zeiss, Oberkochen, Germany). The images were obtained in the Inlens mode at 5 kV. The samples of neat PLA and PLA/PA11 were cryogenically fractured in liquid nitrogen to obtain a cross-section and subsequently sputter-coated with gold (10 mA, 4 min) to create a conductive surface layer of 10 nm.

The average numerical diameter (dn), eq. 1, average volumetric diameter (dv), eq. 2, and dispersion (D), eq. 3, of the diameters of the dispersed phase were determined by measurements on the obtained SEM images, containing more than one hundred 〖(Σ〗_i) dispersed phase particles per sample, according to the following equations:

$$d_n = \frac{\Sigma_i n_i d_i}{\Sigma_i n_i} \tag{1}$$

$$d_v = \frac{\Sigma_i n_i d_i^4}{\Sigma_i n_i d_i^3} \tag{2}$$

$$D = \frac{d_v}{d_n} \tag{3}$$

For particles having ellipse form, an equivalent diameter, eq. 4, was used through the particle area, according to following equation:

$$d_{eq} = 2 \left(\frac{A}{\pi}\right)^{\frac{1}{2}} \tag{4}$$

Differential Scanning Calorimetry (DSC)

The calorimetric analysis was evaluated by differential scanning calorimetry (DSC), using a TA Instruments Q100 in a nitrogen atmosphere on 5 ± 0.5 mg samples sealed in aluminium crucibles. Samples were heated form ambient temperature to 230 °C at 10 °C/min, and held in equilibrium conditions for 3 minutes at 230 °C to eliminate the thermal history, cooled to 25 °C at 10 °C/min, and then reheated to 230 °C at 10 °C/min.

2.4. Photo-Oxidation Exposure

Accelerated photooxidation was carried out using a Q-UV/basic weatherometer (from Q-LAB, USA) equipped with UVB lamps (313 nm). The weathering conditions consist of a continuous light irradiation at T = 70 °C.

3. Results and Discussion

3.1. Effect of ZnO and TiO2 Adding on PLA Properties

As a preliminary study, two different metal oxides, such as zinc oxide (ZnO) and titanium dioxide (TiO2), at different concentrations, i.e., 0.5, 1, and 2wt%, have been added in PLA to establish their effect on solid state properties, melt behaviour and photo-oxidation resistance.

In Table 1, the mechanical properties of PLA and PLA-based systems, i.e., tensile or Young's modulus (E) tensile strength (TS), and elongation at break (EB) at different oxides loading, are reported. The Young's modulus of the PLA/ZnO bio-composite decreased with respect to the pure matrix and as the ZnO contents increased. The results show that adding TiO2, decreases Young's modulus of PLA from 980 MPa to about 745 MPa, and the values exhibit quite values as the oxide content increases. The effect of both oxides on the tensile strength of the neat matrix is almost the same: at lower oxides concentration no relevant change in value was recorded, at high concentrations the values decrease with the same trend for both oxides. Otherwise, the elongation at break of PLA increases in the presence of TiO2 while decreasing in the presence of ZnO.

A proper dispersion of the nanoparticles into the polymer matrix ensures an effective stress transfer from the matrix to the filler and is crucial to obtain a reinforcing effect, while a poor dispersion and the formation of aggregate acting as stress concentrators lead to the weakening of the

mechanical stability. [32] The incompatible nature between the mineral and organic phases and the inherent tendency of oxides nanoparticles to aggregate due to van der Waals interactions and high surface free energy related to the metallic bonds could cause defects in the matrix, reducing the ultimate tensile strength., so the incorporation of ZnO and TiO_2 into a PLA matrix could cause a decrease in the values of TS. Moreover, the ZnO oxide could accelerate the degradation mechanism of PLA during preparation, as confirmed by further analysis, leading to lower molecular weight of the matrix, and worsening the mechanical properties. The effect of the addition of TiO_2 on the thermal stability of PLA during preparation seems to be not impactful; additionally, TiO_2 seems to improve the mobility of matrix chains in the solid state and shows a slight lubricant effect for the PLA matrix.

Table 1 also reported the water contact angle measurements: the presence of metal oxide can modify the surface properties including the hydrophobicity, an important feature in packaging applications since the value of WCA is correlated to the resistance to humidity. The water contact angle measured for neat PLA is 60.1°. The addition of both investigated oxides causes an increase in water contact angle. Anyway, the TiO_2 presence at 2wt% makes the PLA surface more hydrophilic. The surface of titanium dioxide is highly polar, and at high dioxide concentrations, the trend of the contact angle value towards the hydrophobicity can change.

Table 1. Mechanical properties: Young's modulus (E), Tensile Strength (TS), Elongation at Break (EB), Water Contact Angle (WCA) measurements, and crystallinity degree (Δ) of neat PLA, PLA/ZnO and PLA/TiO2 at different contents, i.e., 0.5, 1 and 2 %wt.

samples	E, MPa	TS, MPa	EB, %	WCA, deg	Δ, %
PLA	980 ± 65	34.9 ± 2.5	6.2 ± 0.5	60.10 ± 1.0	9.5
PLA + ZnO at 0.5 %wt	542 ± 52	33.3 ± 3.1	3.5 ± 0.4	65.15 ± 1.2	6.1
PLA + ZnO at 1 %wt	424 ± 45	29.8 ± 3.0	2.9 ± 0.3	70.19 ± 1.3	5.8
PLA + ZnO at 2 %wt	199 ± 22	22.9 ± 3.1	3.6 ± 0.3	78.61 ± 1.2	4.3
PLA + TiO_2 at 0.5 %wt	741 ± 68	35.9 ± 3.4	7.9 ± 0.5	62.64 ± 1.1	6.7
PLA + TiO_2 at 1 %wt	750 ± 69	29.1 ± 3.2	8.7 ± 0.5	65.18 ± 1.2	5.2
PLA + TiO_2 at 2 %wt	744 ± 65	22.5 ± 2.7	9.3 ± 0.6	53.90 ± 1.0	4.8

Rheological characterisation of the system provides information about processability and allows an understanding better how the addition of fillers influences the structure-property relationship. Figure 1 displays the complex viscosity of neat PLA and PLA-based investigated samples. The pure polymer is mainly a linear long-chain structure, so it exhibits a Newtonian behaviour in a wide range of frequencies, and the shear thinning behaviour is observed for angular frequencies greater than 10 rad/s. The incorporation of ZnO at 0.5% and 1% does not cause significant variations while the system PLA/ZnO at 2 %wt shows a higher reduction of the complex viscosity values and more evident no-Newtonian behaviour (Figure 1a). These findings can be related to the decrease in the average molecular weight associated to the degradation of the PLA matrix during preparation due to a huge ZnO presence. [33] Moreover, a dependence of the viscosity on the angular frequency is recorded (Figure 1b).

PLA filled with TiO_2, differently, exhibits a progressive rise in viscosity values concerning those of the neat matrix as the filler concentration increases (Figure 1c) and at lower dioxide contents, the angular frequency dependency is almost negligible, as shown in Figure 1d. The filled systems present an upward shift of the PLA's complex viscosity curve and the onset of shear thinning behaviour slightly moving to higher angular frequency values suggesting that the matrix determines the rheological behaviour and the polymer-polymer interaction is predominant concerning the poor polymer–filler interactions, also according to literature. [34-35] The enhanced melt strength can further infer that the dioxide loading doesn't promote thermal degradation phenomena occurring in PLA processing.
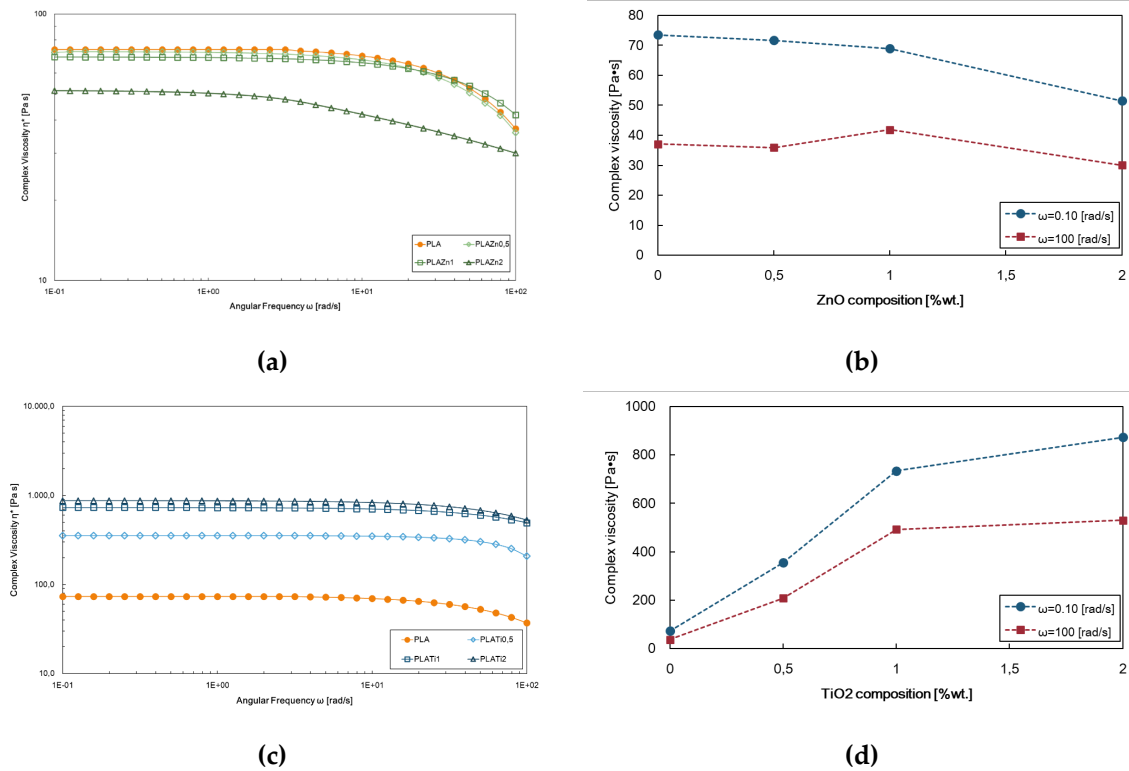
(a)

(b)

(c)

(d)

Figure 1. Rheological analysis, i.e., (a) & (c) complex viscosity and (b) & (d) complex viscosity values at 0.1 and 100 rad/sec of neat PLA, (a-b) PLA/ZnO and (c-d) PLA/TiO$_2$ at different contents, i.e., 0.5, 1 and 2 %wt.

In Figure 2 the height of the peak at 1845 cm-1 for neat PLA and (a) PLA/ZnO and (c) PLA/TiO2 at different contents, i.e., 0.5, 1 and 2 %wt, and selected zone of FTIR spectra of all investigated samples are reported.

According to the literature, the photo-oxidation of PLA is a complex phenomenon that occurs in forming anhydride functions that are detectable as shoulder-to-peak arising at 1845 cm-1. Further, the photo-oxidation behaviour of PLA-based nanocomposites can be also profitably monitored considering the changes of the same peak at 1845 cm^{-1}. [36-37] Considering these notions, the changes of the peak heights at 1845 cm^{-1} are followed for neat PLA and PLA containing different amounts of metal oxides, see Figure 2.

The neat PLA demonstrates excellent durability compared to the samples containing metal oxides. Interestingly, the investigated polymer-metal oxide nanocomposite has a higher degradation rate than that of the pristine matrix related to a superior photodegradation activity under UV light of the filled systems. The pro-degradant effect of both oxides on the polymer matrix increases, as increases the filler amounts, and the degradation progress is faster for PLA/TiO$_2$ than PLA/ZnO also considering that thermal decomposition could occur during the preparation of PLA/ZnO systems. The photo-degradability is affected by the diverse nature of the fillers, which absorb differently the energy and a different dispersion and agglomeration of the fillers in the PLA-based system.
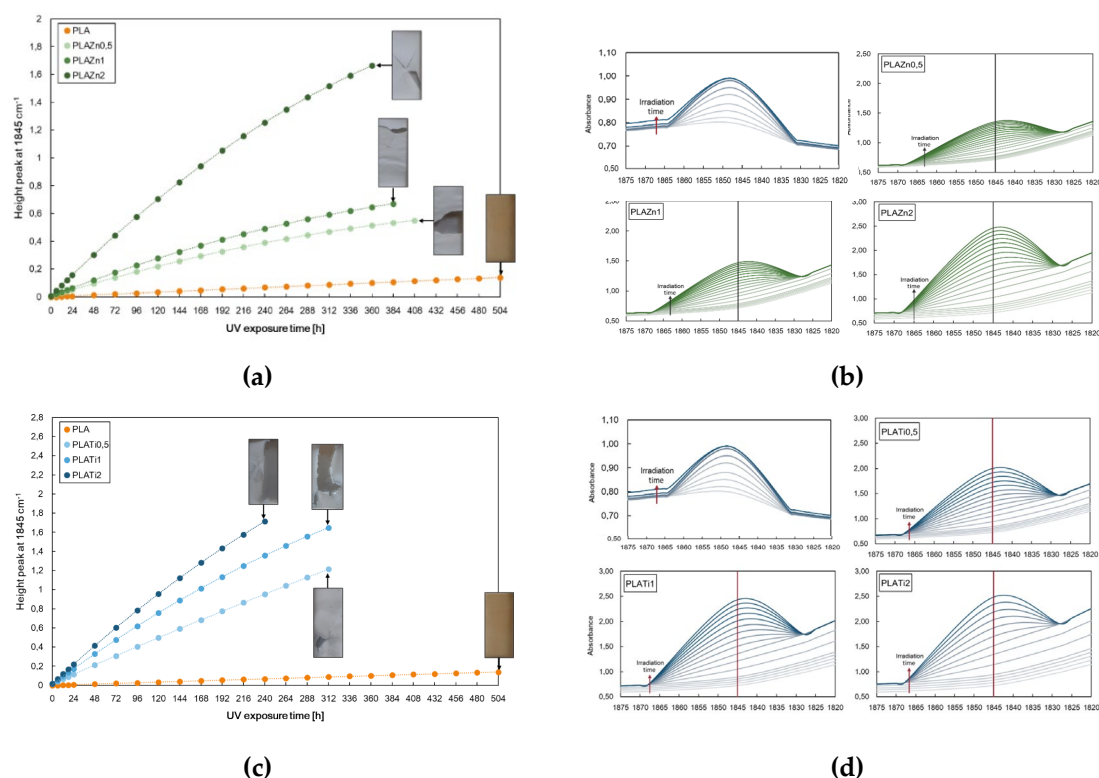
Figure 2. Height of the peak at 1845 cm-1 for neat PLA and (a) PLA/ZnO and (c) PLA/TiO2 at different contents, i.e., 0.5, 1 and 2 %wt., and (b) & (d) selected zone of FTIR spectra of all investigated samples.

Adding to PLA, the 0.5 wt% of ZnO and TiO2 could be considered a thinkable solution because the resultant material exhibits the optimal physical properties, workability, and photodegradability rate to develop commercial products.

3.2. Effect of PA11 Adding on PLA Properties

Polymer blending is a practical and inexpensive approach in which two polymers are combined to achieve superior properties of materials. As reported in the literature, the composing polymers in PLA/PA11 blends exist in separate phases because of immiscibility, so the blend has been intensively studied with the purpose of improving the compatibility of PLA and PA11. [38-42] Here we investigate the effect of the incorporation by melt mixing of different amounts of PA11 in PLA polymer.

Table 2 reports the mechanical properties and water contact angle (WCA) measurements of neat PLA and PA11, and their blends in the analysed composition range: PLA/PA11=85/15, 70/30, 50/50 %wt/wt. The higher elastic modulus of PA11 with respect to PLA is attributed to intermolecular hydrogen bonding in amide groups present in both crystalline and amorphous phases. [41]

The introduction of PA11 in PLA leads to deterioration in the elastic modulus and tensile strength values, and the blends exhibit a non-uniform worsening in mechanical performance with increasing PA11 content in the blends. The EB values of PLA, decrease after the PA11 addition but become higher only for the 50/50 %wt/wt blend. Moreover, the PA11 causes a slight decrease in the surface hydrophilicity of PLA-based blends. The results suggest incompatibility and interfaces unable to successfully transfer the stresses between the polymers, or tensions locally concentrated at defects such as voids. As the dispersion of the PA11 in PLA matrix could influence stress concentrations, later the morphological analysis and a statistical evaluation of the mean diameter of PA11 particles dispersed in the PLA matrix are presented.

Table 2. Mechanical properties, i.e., Young's modulus (E), Tensile Strength (TS), Elongation at Break (EB) and Water Contact Angle (WCA) measurements of neat PLA, neat PA11, and their blends (i.e., PLA/PA11=85/15, 70/30, 50/50 %wt/wt.

samples	E, MPa	TS, MPa	EB, %	WCA, deg
PLA	980 ± 65	34.9 ± 2.5	6.2 ± 0.5	60.10 ± 1.0
PA11	1250 ± 110	19.7 ± 1.5	22.8 ± 2.5	85.3 ± 2.3
PLA/PA11 (85/15 %wt/wt)	632 ± 65	12.7 ± 1.2	2.1 ± 0.3	62.4 ± 1.2
PLA/PA11 (70/30 %wt/wt)	579 ± 54	14.8 ± 1.5	5.0 ± 0.7	64.7 ± 1.0
PLA/PA11 (50/50 %wt/wt)	828 ± 77	21.5 ± 2.1	8.2 ± 0.8	64.7 ± 1.1

The complex viscosities values as a function of angular frequency for neat polymers and investigated blends are reported in Figure 3. The viscosity curve significantly differs between the neat PLA and the neat PA11: as discussed in the previous paragraph, PLA shows a Newtonian behaviour in a wild range of frequency. Conversely, PA11 displays higher values of complex viscosity related to intermolecular interactions and a shear-thinning behaviour in the about whole investigated angular frequency range. At lower PA11 amounts in the blends, PLA seems to govern the rheological behaviour, while at higher PA11 amount, rheological properties of the blend follow those of the dispersed phase, although at higher frequency a more pronounced shear thinning tendency is disclosed. The higher values of the complex viscosity in the low angular frequency range were recorded for the PLA/PA11 (70/30 wt/wt%) blend where the PLA chain mobility decreased; for this blend a more severe viscosity drop is also observed in the high frequency range.
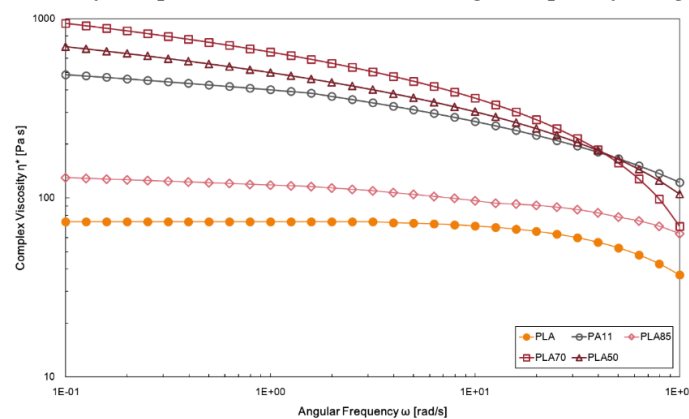

Figure 3. Complex viscosity of neat PLA and PLA/PA11 blends at 85/15, 70/30, 50/50 %wt/wt.

SEM micrographs of PLA/PA11 blends at various magnifications, different compositions, and distribution of PA11 particle dimensions are presented in Figure 4. A drop-matrix morphologies are obtained: the continuous phase is PLA, and the roughly spherical dispersed phase represents PA11. Even supposing PLA/PA11 miscible theoretical solubility, mainly related to the respective low and high polarity, the presence of voids at the PLA/PA11 interface can be noted, so the interface region could be the weakest point in the blend in which failure, leading to fracture, occurs.

A statistical distribution of the dispersed phase size is reported in Figure 4, while in table 3 the average diameter (d_n) of PA11 particles in PLA and ratio (D) between d_n and d_v in PLA/PA11 blends is published. As known, the breakup and coalescence of dispersed droplets take place in polymer blends processing, and at high amounts of PA11, i.e in the PLA/PA11 (50/50 wt/wt%) blend, the droplet coalescence phenomena dominate in PLA matrix and the droplet shape changes from circular to elliptical. In this last event, the extension of the interface region decrease respect to blend containing a lower % of PA11, to minimize the free energy of the system, and the mechanical behaviour is mainly governed by PLA *matrix. Incrementing the PA11 content, the fractured surface shows*

a larger number of holes suggesting that the adhesion between PLA and PA11 is very poor and for this reason, the PLA/PA11=50/50 %wt/wt appears more fragile in comparison to other blends.
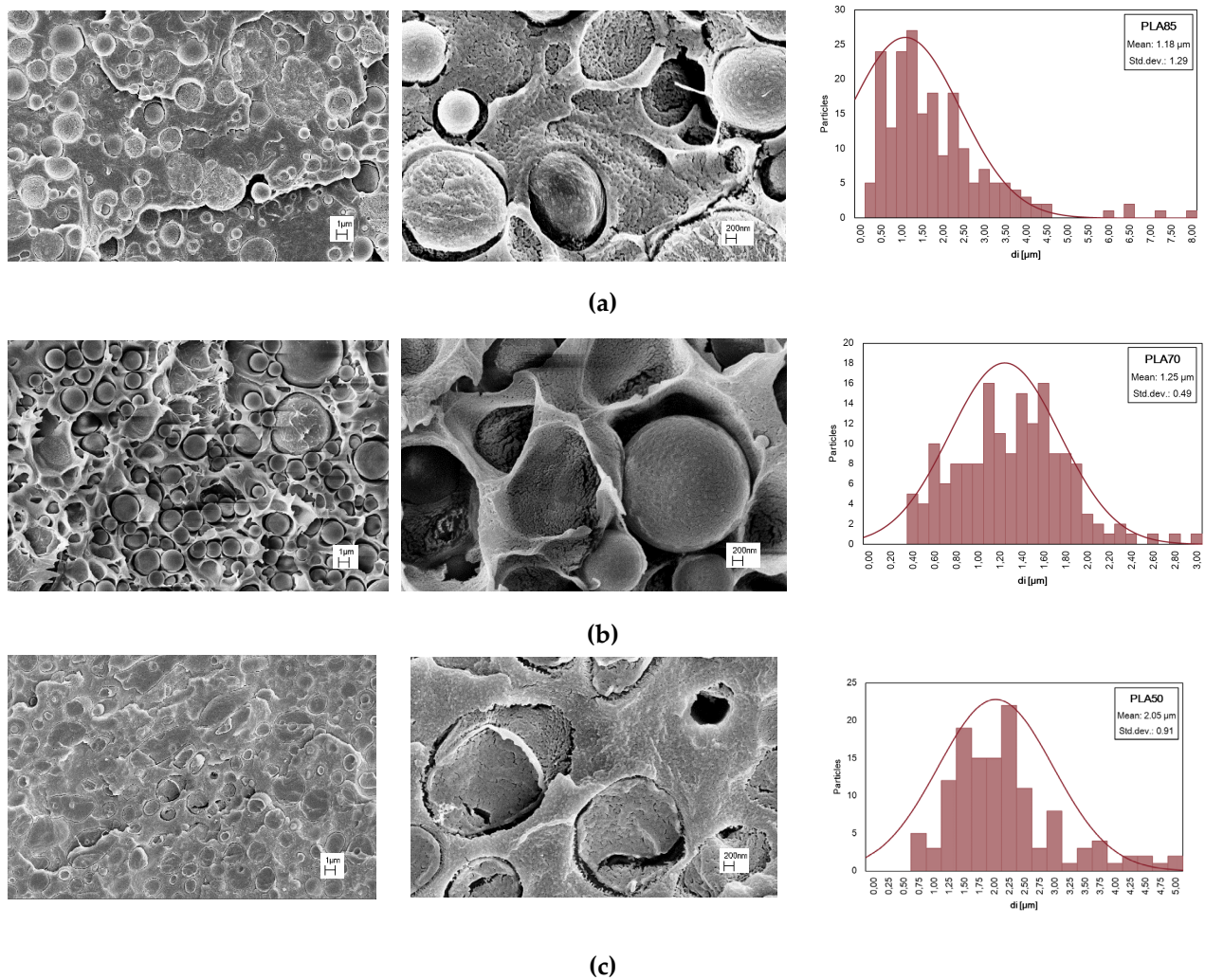

(a)

(b)

(c)

Figure 4. SEM observations at different magnifications and distribution of PA11 particles dimensions of PLA/PA11 blends at (a) 85/15, (b) 70/30, (c) 50/50 %wt/wt.

Table 3. Average dimeter (d_n) of PA11 particles in PLA and ratio (D) between dn and dv in PLA/PA11 blends and blends containing metal oxides, i.e., ZnO and TiO2 at 0.5 %wt.

samples	Σn_i	$d_n\ [\mu m]$	D
(a)			
PLA/PA11 (85/15 %wt/wt)	201	1.28	3.46
PLA/PA11 (70/30 %wt/wt)	166	1.35	1.41
PLA/PA11 (50/50 %wt/wt)	129	2.05	1.65
(b)			
PLA/PA11 (70/30) + ZnO at 0.5 %wt	204	1.02	1.36
PLA/PA11 (70/30) + TiO2 at 0.5 %wt	132	1.57	3.50

The photo-degradation process of PLA and their considered blend were analysed monitoring the progress in the exposure time of 1845 cm^{-1} and 1725 cm^{-1} peaks, linked to the degradation pathway of PLA and PA11 respectively. According to the literature, the PA11 photo-oxidation process can be profitably monitored following the changes in heights of the peak at 1725 cm^{-1} as a

function of UV irradiation time. As known, this peak is assigned to the formation of new oxygen-containing species (e.g. carbonyl and carboxyl functionalities). [43].

PLA, as discussed before, is a durable polymer during UV irradiation and degrades at a higher exposure time than PA11, both photodegrading in the presence of oxygen by αH-abstraction and Norrish I and II photoreactions [41]. At low concentrations of PA11, although the photodegradation rate increases, the specimen endures for almost four weeks of analysis. Conversely, a premature failure of the bio-blends containing higher PA11 concentrations is documented, and the photo resistance decreases as the PA11 amounts increase, as noticeable in Figure 5.

(a)

(b)　　　　　　　　　　　　　　**(c)**
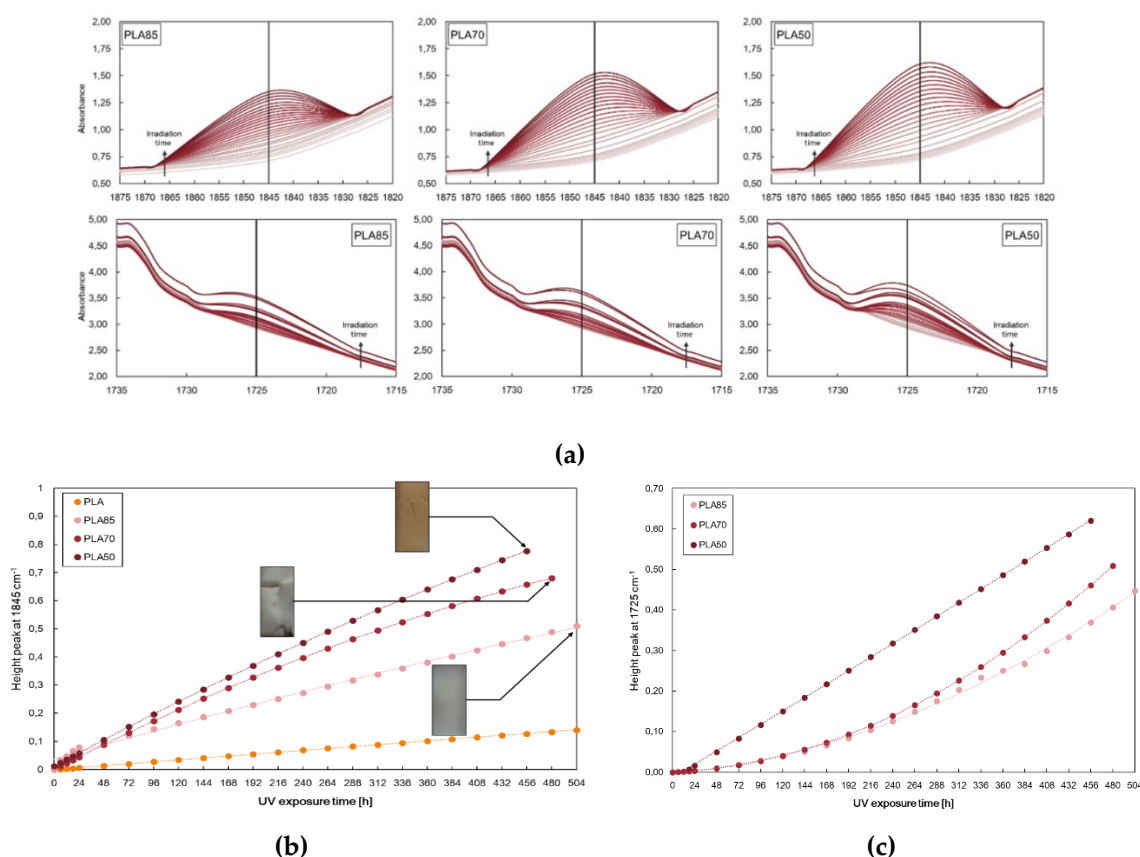
Figure 5. (a) Selected zone in FTIR spectra, (b) height of peak at 1845 cm^{-1} and (c) height of peak at 1725 cm^{-1} of neat PLA and of PLA/PA11 blends at 85/15, 70/30, 50/50 %wt/wt.

Therefore, it seems that the PLA/PA11 blends at 70/30 %wt/wt could be subject to further investigation to obtain materials with designed properties at low cost.

3.3. Effect of ZnO and TiO₂ Adding on PLA/PA11 (70/30 %wt/wt) Properties

Nanoparticles added in a immiscible polymeric blend could enhance the rheological and mechanical properties of the blends, improve the blend morphology and stabilize the dispersed phase against coalescence. [39-41] Therefore, based on above discussed results and our previous experience, there are prepared biopolymer blends at PLA/PA11=70/30 wt/wt% containing ZnO and TiO₂ at 0.5 %wt.

Table 4 reports the mechanical properties of PLA/PA11 blend and PLA/PA11-based blends. PLA/PA11 blend with 0.5 %wt of ZnO shows an improvement in the elastic modulus compared with the blend without oxide, no change in the tensile strength value and a decrease of elongation at break value; the water contact angle is 64.7° for PLA/PA11 (70/30 %wt/wt) blend and decrease to 53,5° for PLA/PA11 (70/30) + ZnO at 0.5 %wt. Conversely, the TiO₂ presence in the blend did not positively influence the mechanical properties, although the elastic modulus value is higher compared to that of the neat blend, and a higher value for WCA is recorded. Results suggest the PA11 phase prevents

the pro-degradant effect of the ZnO on the PLA phase and we can also suppose that ZnO and TiO_2 are more likely at the interface of the dispersed phase.

Table 4. Mechanical properties, i.e., Young 's modulus €, Tensile Strength (TS) and Elongation at Break (EB) and Water Contact Angle (WCA) measurements of PLA/PA11 (70/30 %wt/wt) blend and PLA/PA11 blends containing ZnO and TiO_2 at 0.5 wt%.

samples	E, MPa	TS, MPa	EB, %	WCA, deg
PLA/PA11 (70/30 %wt/wt)	579 ± 54	14.8 ± 1.5	5.0 ± 0.7	64.7 ± 1.0
PLA/PA11 + ZnO at 0.5 %wt	662 ± 63	14.8 ± 1.4	4.4 ± 0.4	53.5 ± 1.2
PLA/PA11+ TiO2 at 0.5 %wt	589 ± 51	9.2 ± 0.9	3.9 ± 0.3	66.7 ± 1.4

Thermograms acquired by calorimetric analysis are reported in Figure 6. PLA cold crystallization temperatures in the neat blend are about at 97.4 and 161.4 °C; after ZnO adding at 0,5 %wt to the blend, no significant changes concerning these temperatures and melting temperatures were observed. A supposed enhanced PLA chain mobility for TiO_2 presence, instead, could cause slightly decreased cold crystallization and melting temperatures and higher crystallinity degree.
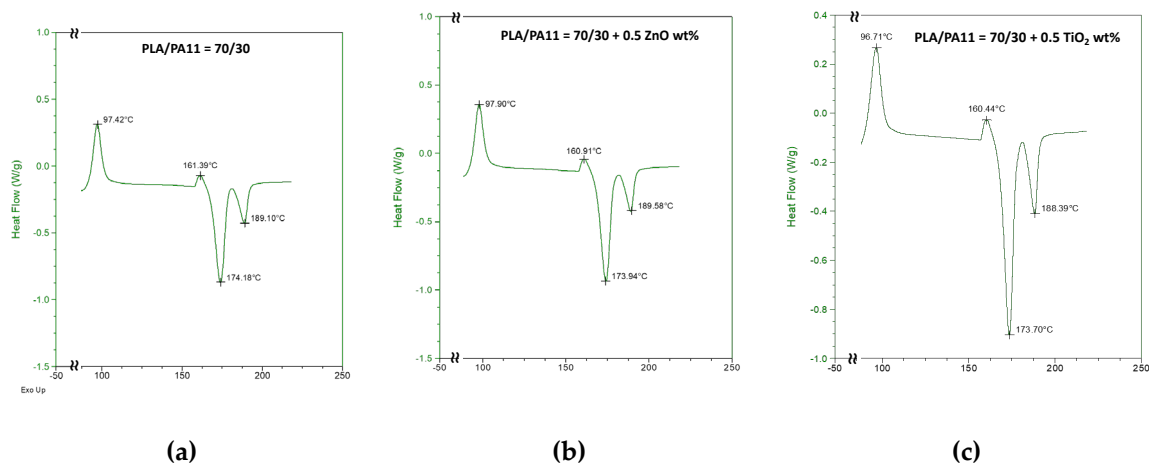

Figure 6. DSC trace of (a) PLA/PA11 (70/30 %wt/wt) blend and PLA/PA11 blends containing (b) ZnO and (c) TiO_2 at 0.5 %wt.

It is crucial to analyze the effect of the nano oxides incorporation on the morphology of the bio blend because of the important effect of the morphology of the blend on the final properties; furthermore, nano oxides could reveal networking ability and promote co-continuity in droplet-matrix morphologies. As expected, after the oxide additions at 0,5% to the blends, the morphology is still droplet-matrix type (Figure 7). Moreover, SEM micrographs point out that no oxide particles were in the continuous phase. The presence of ZnO in the blend led to a PA11 droplet diameter reduction indicating coalescence suppression and increased compatibility between polymers (see Table 3 and Figure 7a). We can note that PA11 dispersed phases diameter seems to increase with respect to the neat blend after TiO2 introduction and the narrowing of the size distribution is observed, as reported in Figure 7b.
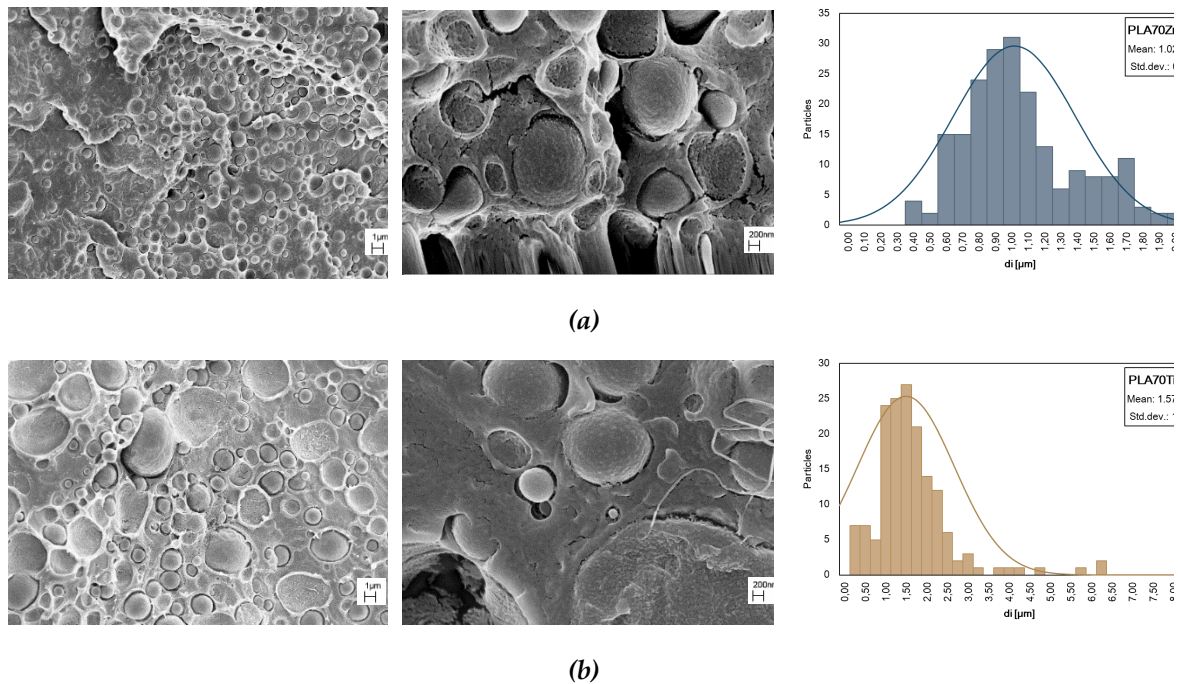
(a)

(b)

Figure 7. SEM observations at different magnifications and distribution of PA11 particles dimensions of PLA/PA11 blends containing (a) ZnO and (b) TiO₂ at 0.5 %wt.

Figure 8 illustrates the complex viscosity η*, the storage modulus G' and the loss modulus G" versus angular frequency of neat PLA/PA11 (70/30) blend and PLA/PA11 blends containing ZnO and TiO2 at 0.5 %wt. The viscosity values of the PLA/PA11 (70/30) + ZnO at 0.5 wt% and of the PLA/PA11 (70/30) + TiO2 at 0.5 %wt exceed those of the neat blend. In contrast to what was previously observed, the ZnO presence doesn't cause lower complex viscosity of PLA because the PA11 presence prevents thermo-oxidative degradation during preparation. The blend containing TiO₂ shows a similar viscosity curve to that of neat PLA. The Newtonian plateau of PLA/PA11 (70/30 %wt/wt) + TiO₂ at 0.5 %wt is observed in a wider frequency range compared to the neat blend, moreover at low frequency, the loaded blend exhibits a weak yield behaviour compared to the neat blend as a result of weak intermolecular force.

The rheological response of the storage modulus against the angular frequency of the investigated samples is illustrated in Figure 8(b). The presence of both metal oxides in the blend enhances the modulus of the melts, indicating a reinforcing effect. The storage modulus for all samples is independent of the frequency in the low-frequency region, showing a solid-like behaviour attributed to polymer interactions in the polymer matrix. Results obtained from rheological analysis suggest that the rheological behaviour is mainly governed by PLA matrix. Moreover, the enhancement of the rheological properties seems to confirm affinity of both oxides towards the PA11 phase and the shielding effect of polyamide on PLA degradation against the pro-degradant action of metal oxide.
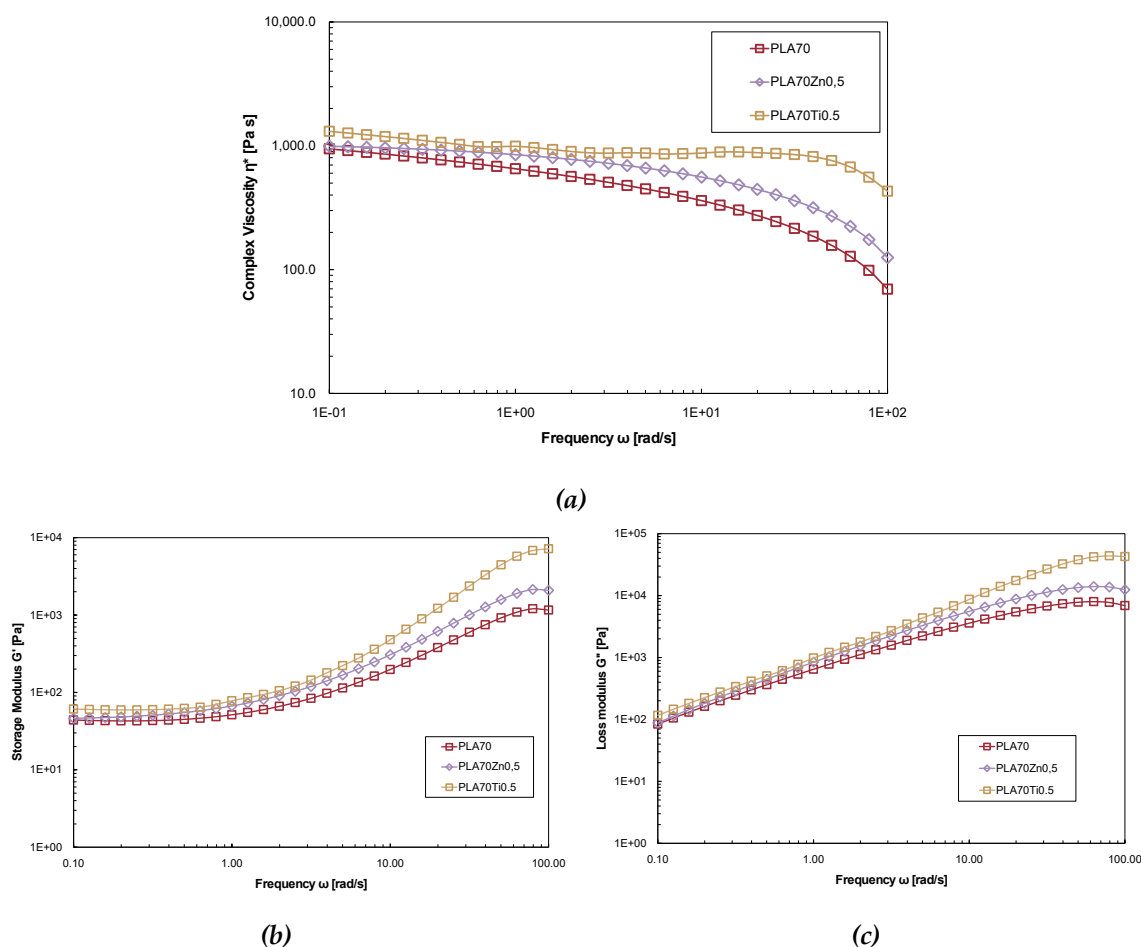
(a)

(b)

(c)

Figure 8. Complex viscosity (a) the storage modulus G'(b) and the loss modulus G'' (c) of neat PLA/PA11 (70/30 %wt/wt) blend and PLA/PA11 blends containing ZnO and TiO2 at 0.5 %wt.

The effect of the investigated metal oxides upon the UV irradiation depends on their distribution in the polymer matrix, in particular can act as pro-degradants leading to a reduction in polymer molecular weight or can act as protecting agents, shielding the UV irradiation. [44-45] Morphological, rheological, and mechanical analysis suggest that both oxides are tendentially localised in the PA11 phase or at the interface between PLA and PA11 so avoiding the ZnO pro-degradation effect on PLA matrix. Anyway, we have to take into account that higher filler loadings could exceed a segregation limit in PA11 drops, causing their exposure toward the PLA phase. The PLA/PA11 blends containing ZnO and TiO$_2$ at 0.5 %wt. show a very interesting photo-oxidation behaviour and it was monitored again following the changes in both peaks at 1845 cm^{-1} and 1725 cm^{-1}, related to the degradation pathways of PLA and PA11, respectively. Monitoring the height peak at 1845 cm^{-1}, we can assert that the photodegradation rate of the PLA, in terms of accumulation of anhydride functionalities, decreases in the presence of the blend of both ZnO and TiO2 nanoparticles. On the contrary, the trends of the height of the peak at 1725 cm^{-1} show opposite trends, resulting in accelerated photodegradation of PA11, in terms of accumulation of oxygen-containing groups. The latter confirms that both ZnO and TiO$_2$ are located preferentially in the more polar polyamide phase, causing its accelerated photodegradation. Worth noting that both oxides cause a short lifetime of the obtained bio-blends. The PLA/PA11/ZnO and PLA/PA11/TiO$_2$ become brittle only after 384 h and 288 h of UV irradiation for ZnO and TiO$_2$, respectively, in comparison to 480 h requested for neat PLA, and for this reason, the FTIR analyses have been interrupted, as noticeable in Figure 9.
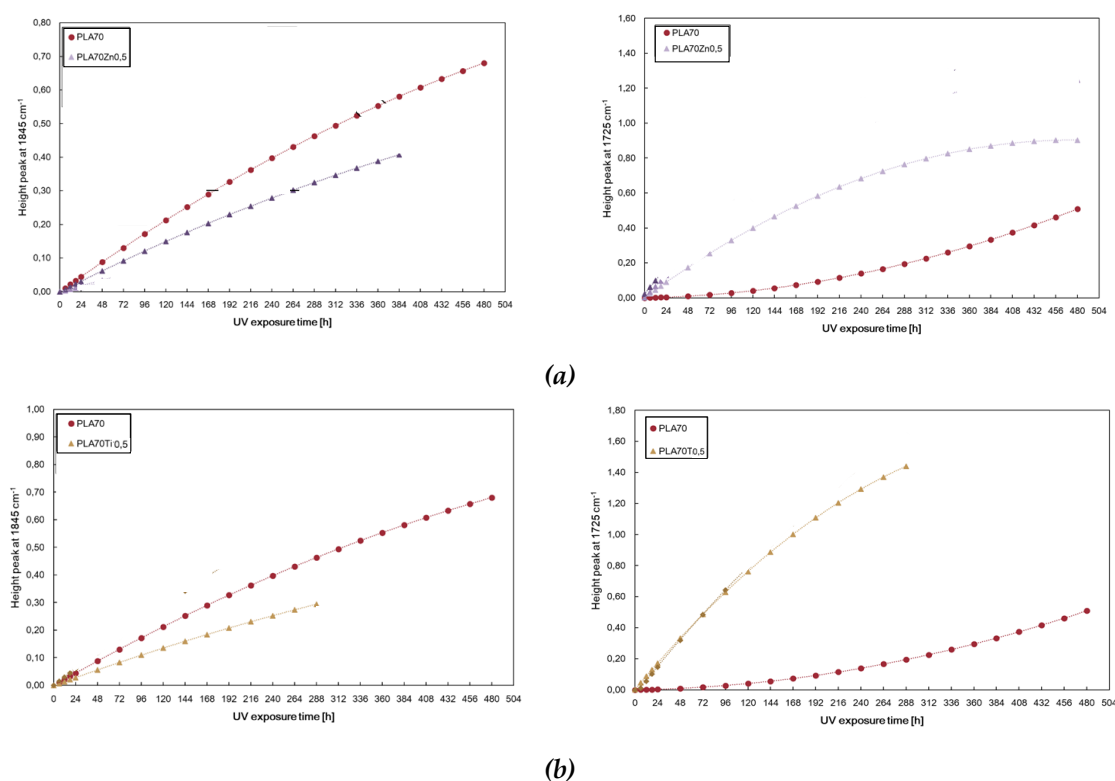
(a)

(b)

Figure 9. Photo-oxidation behaviour of neat PLA/PA11 (70/30) blend and PLA/PA11 blends containing (a) ZnO and (b) TiO$_2$ at 0.5 %wt.

5. Conclusions

The properties of the biopolymer and biopolymer blends-based nanocomposites are predominantly influenced by the individual nature of the constituents and the interface between them and by the concentration, size and shape of the particles, and the morphology of the resultant system.

This work has demonstrated that the incorporation of the metal oxides in the PLA-based matrices, although not desirable for the mechanical properties, improves the degradation efficiency of the nanocomposites, leading to a lower residence time of the resulting waste in the environment. Both zinc oxide and titanium dioxide cause a significant reduction of the PLA photo-oxidation resistance, although their presence slightly increases the PLA hydrophobicity, and the latter suggests that the PLA hydrolysis could be slowed down.

The PLA-based blends, e.g. PLA/PA11, show predominantly globular morphology that can be modified and refined by the presence of metal oxides up to ellipsoid morphology due to the preferential location of the particle in the more polar polyamide phase. Interestingly, the PLA/PA11 blends containing ZnO and TiO$_2$ show slowed down accumulation of anhydride species, coming from the oxidation of PLA, and accelerated accumulation of oxygen-containing groups, coming from the degradation of PA11. The latter could be considered indirect evidence of the preferential location of the metal oxide particles in the more polar polyamide phase.

The presence of both metal oxides has beneficial effects, although less pronounced, on the solid-state properties of PLA/PA11 blend helping the formulation of biopolymer-based materials with modulated and tuned properties and performance.

These findings aim to enlarge the use of PLA-based blends and composites and it suggest that further investigations such as a compatibilizer presence or a functionalization of the metal oxides particles are required to improve and optimize the system morphology and properties.

Supplementary Materials: Not supporting information.

15

References

1. Siva Prasanna, S.R.V.; Balaji, K.; Pandey, Sh.; Rana, S. Chapter 4 - Metal Oxide Based Nanomaterials and Their Polymer Nanocomposites, In "Nanomaterials and Polymer Nanocomposites", Karak, N. Ed.; Elsevier, 2019; pp. 123-144, ISBN 9780128146156, https://doi.org/10.1016/B978-0-12-814615-6.00004-7

2. Nikolaeva, A.L.; Bugrov, A.N.; Sokolova, M.P.; Ivan'kova, E.M.; Abalov, I.V.; Vlasova, E.N.; Gofman, I.V. Metal Oxide Nanoparticles: An Effective Tool to Modify the Functional Properties of Thermally Stable Polyimide Films. *Polymers* 2022, 14, 2580. doi: 10.3390/polym14132580

3. Ahmed, B.; Singh, A.; Ushal, R.; Yusuf, M.; Kumar, S.; Kumar Ojha, A.; Khanf W. "Overview of Polymer/Metal-Oxide Nanocomposites: Synthesis, Properties, and Their Potential Applications." In "Handbook of Nanofibers and Nanocomposites". Yusuf, M.; Haji, A. Ed.s; Jenny Stanford Publishing, 1st ed.; 2024; pp. 193-220. ISBN: 9781003432746

4. Zarrintaj, P.; Khalili, R.; Vahabi, H.; Reza Saeb, M.; Reza Ganjali, M.; Mozafari, M. Chapter 8 – "Polyaniline/metal oxides nanocomposites", In "Fundamentals and Emerging Applications of Polyaniline", Mozafari, M.; Singh Chauhan, N.P. Ed.s; Elsevier, 2019, pp. 131-141, ISBN 9780128179154, https://doi.org/10.1016/B978-0-12-817915-4.00008-7

5. Opoku, F.; Kiarii, E.M.; Govender, P.P.; Mamo, M.A. "Metal Oxide Polymer Nanocomposites in Water Treatments", In: "Descriptive Inorganic Chemistry Researches of Metal Compounds", Akitsu, T. ed.; IntechOpen, Rijeka, 2017 https://doi.org/10.5772/67835

6. Velempini, T.; Prabakaran, E.; Pillay, K. "Recent developments in the use of metal oxides for photocatalytic degradation of pharmaceutical pollutants in water—a review", *Materials Today Chemistry*, 2021, 19, 100380. doi: 10.1016/j.mtchem.2020.100380

7. Danish, M.S.S.; Bhattacharya, A.; Stepanova, D.; Mikhaylov, A.; Grilli, M.L.; Khosravy, M.; Senjyu, T. A. "Systematic Review of Metal Oxide Applications for Energy and Environmental Sustainability". *Metals* 2020, 10, 1604. doi: 10.3390/met10121604

8. Amini, M.; Ashrafi, M. "Photocatalytic degradation of some organic dyes under solar light irradiation using TiO2 and ZnO nanoparticles". Nano Chem Res. 2016, 1, 79–86. doi: 10.7508/NCR.2016.01.010

9. Le, A.T.; Pung, S.; Sreekantan, S.; Matsuda, A.; Huynh, D.P. Mechanisms of removal of heavy metal ions by ZnO particles. Heliyon 2019, 5, e01440. doi: 10.1016/j.heliyon.2019.e01440

10. Alardhi, S.M., Abdalsalam, A.H., Ati, A.A. et al. Fabrication of polyaniline/zinc oxide nanocomposites: synthesis, characterization and adsorption of methylene orange. *Polym. Bull.* 81, 2024, 1131–1157. https://doi.org/10.1007/s00289-023-04753-1

11. Yadav, H.M.; Kim, J.-S.; Pawar, S.H. "Developments in photocatalytic antibacterial activity of nano TiO2: a review", Kor. J. Chem. Eng. 2016, 33, 1989-1998. doi: 10.1007/s11814-016-0118-2

12. Pachaiappan, R.; Rajendran, S.; Loke Show, P.; Manavalan, M.; Naushad, M. "Metal/metal oxide nanocomposites for bactericidal effect: A review", *Chemosphere*, 2021, 272. doi: 10.1016/j.chemosphere.2020.128607

13. Akira Fujishima, A,; Rao, T.N.; Tryk, D.A. "Titanium dioxide photocatalysis", *J. Photochem. Photobiol. C: Photochemistry Reviews*, 2000, 1, 1-21. doi: 10.1016/S1389-5567(00)00002-2

14. Barnes, D.K.; Galgani, F.; Thompson, R.C.; Barlaz, M. "Accumulation and fragmentation of plastic debris in global environments". *Philos. Trans. R. Soc. Lond. B Biol. Sci.* 2009, 364(1526), 1985-1998. doi: 10.1098/rstb.2008.0205.

15. Borriello, L.; Scivicco, M.; Cacciola, N.A.; Esposito, F.; Severino, L,.; Cirillo, T. "Microplastics, a Global Issue: Human Exposure through Environmental and Dietary Sources". *Foods.* 2023 Sep 11;12(18):3396. doi: 10.3390/foods12183396.

16. Ravanchi, M.T.; Soleimani, M. "Global warming and greenhouse effect resulted from oil, gas, and petrochemical units", In "Crises in Oil, Gas and Petrochemical Industries", Rahimpour, MR.; Omidvar, B.; Shirazi, N.A.; Makarem, M.A. eds. Elsevier, 2023, pp. 257-282. doi: 10.1016/B978-0-323-95154-8.00002-5

17. Santos, A.; Barbosa-Póvoa, A.; Carvalho, A. "Life cycle assessment in chemical industry – a review", *Current Opinion in Chem. Eng.*, 2019, 26, 139-147, ISSN 2211-3398. doi: 10.1016/j.coche.2019.09.009

18. Steinbüchel, A. "Non-biodegradable biopolymers from renewable resources: perspectives and impacts", Current Opinion in Biotechnology, 2005, 16, 607-613, ISSN 0958-1669. doi: 10.1016/j.copbio.2005.10.011

19. Das, A.; Ringu, T.; Ghosh, S.; Pramanik, N. "A comprehensive review on recent advances in preparation, physicochemical characterization, and bioengineering applications of biopolymers". *Polym. Bull.* 2023, 80, 7247–7312. doi: 10.1007/s00289-022-04443-4

20. Hanifah, A.; Mahardika, M. A., Sumirat, R., Nissa, R.C., Nurhamiyah, Y. Recent Updates on Biopolymers: Precursors, Process, Properties, Challenge, and Future Perspectives. In: Biomass Conversion and Sustainable Biorefinery. Lubis, M.A.R., et al. 2024. Green Energy and Technology. Springer, Singapore. https://doi.org/10.1007/978-981-99-7769-7_2

21. Taib, NA.A.B., Rahman, M.R., Huda, D. et al. A review on poly lactic acid (PLA) as a biodegradable polymer. *Polym. Bull.* 2023, 80, 1179–1213. doi: 10.1007/s00289-022-04160-y

22. Park, S.B.; Lih, E.; Park, K.S.; Joung, Y.K.; Han, D.K. "Biopolymer-based functional composites for medical applications". *Prog Polym Sci* 2017, 68, 77–105. doi: 10.1016/j.progpolymsci.2016.12.003

23. Kulkarni, R.K.; Moore, E.G.; Hegyeli, A.F.; Leonard, F. "Biodegradable poly(lactic acid) polymers". *J Biomed Mater Res.* 1971 May;5(3):169-81. doi: 10.1002/jbm.820050305

24. NatureWorks LLC Announces World's First Greenhouse-GasNeutral Polymer, 2005

25. Bikiaris, N.D.; Koumentakou, I.; Samiotaki, C.; Meimaroglou, D.; Varytimidou, D.; Karatza, A.; Kalantzis, Z.; Roussou, M.; Bikiaris, R.D.; Papageorgiou, G.Z. Recent Advances in the Investigation of Poly(lactic acid) (PLA) Nanocomposites: Incorporation of Various Nanofillers and their Properties and Applications. *Polymers,* 2023, 15, 1196. doi: 10.3390/polym15051196

26. Sharif, A.; Mondal, S.; Hoque, M.E. "Polylactic acid (PLA)-based nanocomposites: Processing and properties". In: Bio-based Polymers and Nanocomposites. Springer, Cham, 2019. pp. 233-254

27. Sanyang, M.L.; Jawaid, M. ed.s, Bio-based Polymers and Nanocomposites: Preparation, Processing, Properties & Performance. Springer, 2019.

28. Stoclet, G.; Seguela, R.; Lefebvre, J.-M. "Morphology, thermal behavior and mechanical properties of binary blends of compatible biosourced polymers: Polylactide/polyamide11", *Polymer,* 2011, 52, 1417-1425. doi: 10.1016/j.polymer.2011.02.002

29. Patel, R.; Ruehle, D.A.; Dorgan, J.R.; Halley, P.; Martin, D. "Biorenewable blends of polyamide-11 and polylactide". *Polym. Eng. Sci.* 2013, 54, 1523-1532. doi: 10.1002/pen.23692

30. Shen, L.; Haufe, J.; Patel, M.K. "Product overview and market projection of emerging bio-based plastics PRO-BIP 2009. Report for European polysaccharide network of excellence (EPNOE) and European bioplastics", 2009, 243. https://plasticker.de/docs/news/PROBIP2009_Final_June_2009.pdf

31. Puglisi, R.; Scamporrino, A.A.; Dintcheva, N.T.; Filippone, G.; Bruno, E.; Scarfato, P.; Cerruti, P.; Carroccio, S.C. Photo- and Water-Degradation Phenomena of ZnO Bio-Blend Based on Poly(lactic acid) and Polyamide 11. Polymers 2023, 15, 1434. https://doi.org/10.3390/polym15061434

32. Nielsen, L.; Landel, R. "Mechanical Properties of Polymers and Composites", Marcel Decker, New York, USA, 1994.

33. Murariu, M.; Doumbia, A.; Bonnaud, L.; Dechief, A.L.; Paint, Y.; Ferreira, M.; Campagne, C.; Devaux, E.; Dubois, P. "High-Performance Polylactide/ZnO Nanocomposites Designed for Films and Fibers with Special End-Use Properties", *Biomacromolecules* 2011, 12, 1762–1771. doi: 10.1021/bm2001445

34. Arrigo, R.–Bartoli, M.; Malucelli, G. Poly(lactic Acid)–Biochar Biocomposites: Effect of Processing and Filler Content on Rheological, Thermal, and Mechanical Properties. *Polymers* 2020, 12, 892. doi: 10.3390/polym12040892

35. Botta, L.; Scaffaro, R.; La Mantia, F.P.; Dintcheva, N.Tz. "Effect of different matrices and nanofillers on the rheological behavior of polymer-clay nanocomposites" *J. Polym. Sci. B Polym. Phys*., 2010, 48, 344-355. doi: 10.1002/polb.21896

36. Gardette, M.; Thérias, S.; Gardette, J-L.; Murariu, M.; Dubois, P. "Photooxidation of polylactide/calcium sulphate composites", Polym. Degrad. Stab., 2011, 96, 616-623. doi: 10.1016/j.polymdegradstab.2010.12.023

37. Pérez Amaro, L.; Cicogna, F.; Passaglia, E.; Morici, E.; Oberhauser, W.; Al-Malaika, S.; Dintcheva, N.Tz.; Coiai, S. "Thermo-oxidative stabilization of poly(lactic acid) with antioxidant intercalated layered double hydroxides" *Polym. Degrad. Stab.* 2016, 133, 92-100, doi: 10.1016/j.polymdegradstab.2016.08.005

38. Yu, X.; Wang, X.; Zhang, Z.; Peng, S.; Chen, H.; Zhao, X. "High-performance fully bio-based poly(lactic acid)/ polyamide11 (PLA/PA11) blends by reactive blending with multi-functionalized epoxy", *Polymer Testing,* 2019, 78, 105980. doi: 10.1016/j.polymertesting.2019.105980

39. Rasselet, D.; Caro-Bretelle, A.-S.; Taguet, A.; Lopez-Cuesta, J.-M. "Reactive Compatibilization of PLA/PA11 Blends and Their Application in Additive Manufacturing". *Materials* 2019, 12, 485. https://doi.org/10.3390/ma12030485

40. Khankrua, R.; Wiriya-Amornchai, A.; Triamnak, N.; Suttiruengwong, S. "Biopolymer blends based on poly(lactic acid) and polyamide for durable applications", *Polymer-Plastics Technol. Mater.* 2023, 62, 131-144, doi: 10.1080/25740881.2022.2096470

41. Nuzzo, A.; Coiai, S.; Carroccio, S.C.; Dintcheva, N.Tz.; Gambarotti, C.; Filippone G. "Heat-resistant fully bio-based nanocomposite blends based on Poly(lactic acid)" *Macromol. Mater. Eng.* 2014, 299, 31-40. doi: 10.1002/mame.201300051

42. Dintcheva, N.Tz.; Filippone, G.; La Mantia, F.P.; Acierno D. "Photo-oxidation behaviour of polyethylene/polyamide 6 blends filled with organomodified clay: Improvement of the photo-resistance through morphology modification" *Polym. Degrad. Stab*, 2010, 95, 527-535. doi: 10.1016/j.polymdegradstab.2009.12.021

43. Dintcheva, N.Tz.; Al-Malaika, S.; Morici, E. "Novel organo-modifier for thermally-stable polymer-layered silicate nanocomposites" *Polym. Degrad. Stab.* 2015, 122, 88-101. doi: 10.1016/j.polymdegradstab.2015.09.005

44. Rasouli, D.; Dintcheva, N.Tz.; Faezipour, M.; La Mantia, F.P.; Farahani, M.R.M.; Tajvidi, M. "Effect of nano zinc oxide as UV stabilizer on the weathering performance of wood-polyethylene composite" *Polym. Degrad. Stab.,* 2016, 133, 85-91. doi: 10.1016/j.polymdegradstab.2016.08.004

45. Grigoriadou, I.; Paraskevopoulos, K.M.; Chrissafis, K.; Pavlidou, E.; Stamkopoulos, T.-G.; Bikiaris, D. "Effect of different nanoparticles on HDPE UV stability", *Polym. Degrad. Stab.,* 2011, 96, 151-163, doi: 10.1016/j.polymdegradstab.2010.10.001